Bulletin of the Earthquake
Research Institute
University of Tokyo
Vol. 60 (1985) pp. 1-21

Mechanical Interaction between Neighboring Active Faults —Static and Dynamic Stress Field Induced by Faulting—

Kacper Rybicki*, Teruyuki Kato and Keichi Kasahara

Earthquake Research Institute, University of Tokyo

(Received March 14, 1985)

Abstract

The seismic disturbances that a potentially active fault receives from a slip on a neighboring fault might be considered as nature's mechanical stability. The problem of static and dynamic stress fields induced by faulting is analysed as a way to estimate the stability of nearby active faults. The source fault is modelled by a Volterra dislocation of a strike-slip type along a vertical surface embedded in an elastic homogeneous infinite medium for both dynamic and static models. In order to represent quantitatively a resultant effect of stress caused by the source fault, a new scalar quantity is introduced in reference to the results of laboratory studies on fault friction. This quantity, which is called the resultant stress, is the linear combination of shear and normal components of the induced stress vector acting on the potential fault which is assumed to be parallel to the source fault. The spatial distribution of the static resultant stress in the seismogenic layer, which was calculated in the semiinfinite medium, indicates four regions around the source where the resultant stress takes positive values. These regions extend from the fault surface and in the direction close to the strike of the fault. The probability of further fracture in these regions increases as a result of stress redistribution in the medium due to faulting. The dominant characteristics of the dynamic stress field is the strong directivity effect, which is especially apparent in the case of a unilateral rupture. The correlation between the static and the dynamic field is also notable. The maximum values of the dynamic resultant stress are of the order of 10 bars at distances comparable to fault dimensions, if we assume a fault model which is equivalent to a M7.0 earthquake. The ratio of maximum dynamic stress to the corresponding static stress takes the values ranging from a few to 50 bars or more, depending on the location of an observer and the character of rupture propagation. This means that if a potentially active fault is located in the vicinity of a seismic source, then it could be loaded with high dynamic stress whose peak value would be equivalent to tens of years of stress ac-

* On leave from the Institute of Geophysics, Polish Academy of Sciences.

cumulation at a normal tectonic rate. Such interpretation, however, must be checked carefully with respect to the time-dependence effect of applied stress on material strength.

1. Introduction

During the last few decades, substantial progress has been made in the understanding of mechanical processes taking place in seismotectonic areas. The seismic area is generally thought to accumulate regional tectonic stress, which increases in time and eventually releases its energy by occasional fractures (fault slips) at such localities where the stress has reached the strength of rocks. Fractures in the crust tend to recur along the surfaces of previous fractures which are of relatively low strength. Consequently, in the long run, a group of active faults becomes predominant in the area.

Suppose that one of the active faults slips, then other neighboring potentially active faults will receive seismic disturbances from the source fault in the form of dynamic stress waves (transient effect) and also in the form of permanent residual stress. (Static stress changes are in fact zero frequency seismic disturbances.) It is obvious that these seismic disturbances will more or less affect the succeeding fractures in the area. Even from such a rather schematic and brief description of seismotectonic sequences it becomes clear that the knowledge of mechanical interaction between neighboring active faults should be useful for the better understanding of crustal dynamics, in general, and for long-term earthquake prediction, in particular.

The problem of static stress changes due to faulting has already been studied and applied to various problems of geophysical interest (e.g. CHINNERY, 1963, 1966a, b; SMITH and VAN DE LINDT, 1969; YAMASHINA 1978; DAS and SCHOLZ, 1981; STEIN and LISOWSKI, 1983; NIEWIADOMSKI and RYBICKI, 1984). In this paper we deal with the problem of stress fields induced by faulting in relation to the question of how this field affects the stability of adjacent faults. New elements of the present analysis may be characterised as follows: (1) simultaneous consideration of static and dynamic stress fields, (2) the range of depth at which the stress field is considered comparable to that of the seismogenic layer, and (3) both shear and normal stress components are taken into account using the results of laboratory experiments concerning friction on a fault (similar approaches with respect to the third point above have been take by some other researchers as well, e.g. CHINNERY, 1966a, SAVAGE and CLARK, 1982; STEIN and LISOWSKI, 1983; STEIN,

1984). To summarize, this paper aims at a better understanding of the problem of stability of an active fault by analysing the basic features of seismic disturbances caused by a movement on a neighboring fault.

There are several major seismic zones for which the problem of fault interaction is of great practical importance, e.g. the San Andreas (California), Anatolia (Turkey), and Alpine (New Zealand) fault systems. The model analysed in the present paper, however, is meant to represent a rather local seismically active region in central Honshu, Japan. This area extends approximately 200 km × 200 km, and has a fairly uniform distribution of active faults whose orientation suggests the existence of a persistent tectonic stress of east-west compression. Its seismotectonic characteristics, regarding the past and on-going activities, are fairly well known from geological, geodetic, geophysical and seismological reports as well as from historical documents (e.g. RESEARCH GROUP FOR ACTIVE FAULTS, 1980). This is a typical intra-plate seismic area. The Atera fault, which is the principal fault located approximately in the central part of the area, is ranked as a class A inland active fault, which means that the geological slip rate is 1–10 mm/yr. This fault, however, has not moved for more than the past one thousand years, which is almost close to its average recurrence period as inferred from geological data (e.g. MATSUDA, 1977). This is the main reason for selecting the present region in our analysis.

2. Model

Let us assume the occurrence of a magnitude 7 earthquake adjacent to the Atera fault and study its seismic disturbances (in fact, the present area has released several earthquakes of magnitude 6–7 in the last several decades). Consider a left-lateral strike-slip fault intersecting the free surface in the Cartesian coordinate system (x, y, z), where the x-axis is directed along the strike of the fault, the y-axis is perpendicular to it and the z-axis points downward (Fig. 1a). Assume that, under the action of shear tectonic stress, the rupture initiate at depth D and a circular rupture front advances from the hypocenter with a constant rupture velocity v until it covers a rectangular fault surface of length L and of width W. The source time function $\Delta u_x(t)$ is of the ramp-type with a rise time of t_0. Δu_x is assumed to be uniform over the fault plane so that the final slip along the fault, $\Delta u_x(t>t_0)=b$, is also uniform.

For the fault model as described above, we computed the dynamic and static stress due to faulting, assuming that the fault is embedded

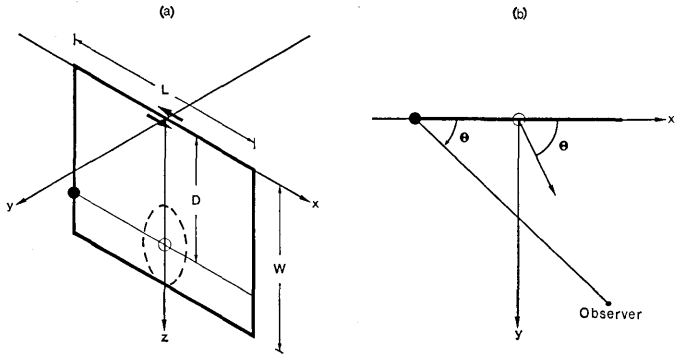

Fig. 1. Geometry of the model analysed. (a) A vertical strike-slip fault of length L and of width W is located in the plane $y=0$. The rupture (● unilateral rupture, ○ bilateral rupture) initiates at depth D and propagates radially. (b) The cross section in a plane $z=$const. θ is the angle between the x-axis (strike-slip direction) and the line joining an observation point with the initial point of rupture.

in an infinite homogeneous medium with P- and S- wave velocities equal to v_P and v_S, respectively. The dynamic stress was computed using the fast computation technique and the computer program, both developed by SATO (1975, 1976) and IWASAKI (1978). Calculations of the static stress field due to faulting were made by the computer program written by IWASAKI and SATO (1979).

Let us specify the adjacent potentially active fault to be parallel to the source fault (i.e. the normal to the surface of the potential fault is also in the y-direction). Then we need to calculate only three components S_{xy}, S_{yy}, and S_{zy} of the stress tensor $S_{ij}(i, j=1, 2, 3)$ to represent the stress vector acting across the specified surface. For a reason which will be explained later, an additional quantity called the "resultant stress" which involves S_{xy}, and S_{yy} components was introduced and calculated. (STEIN (1984) also introduced a similar quantity.) In order to get the three-dimensional distribution of these four components, the computations were performed for different observation points located around the fault in horizontal planes at various depths below the ground surface (Fig. 1b).

We assumed the following values of the parameters describing the model under consideration: $v_P=5.6$ km/s, $v_S=3$ km/s, $v=0.9$ $v_S=2.7$ km/s, $t_0=2$s, $b=1.6$ m, $W=15$ km, $L=20$ km, $D=10$ km. Such values of the parameters would simulate a seismic event of magnitude $M=7$, in reference to the empirical formula proposed by MATSUDA (1975). The location of the hypocenter, i.e. the point of first breakage, is critical in respect to the dynamic stress field. In the present calculation,

therefore, two extreme cases are considered. In the first case the initial point of rupture is located at point $(0, 0, D)$, which is the case of bilateral symmetric rupture, while in the second case the rupture starts from point $(-L/2, 0, D)$, which represents the case of unilateral rupture. The present set of parameters is only provisional and should be adjusted carefully for a more realistic model of fault interaction. Still such a simplified model is useful to study the general features of the phenomenon.

3. Results

a. Static stress in the infinite medium

The stress components S_{xy}, S_{yy} and S_{zy} were computed at the following horizontal planes $z=0$ (ground surface), $z=5$, $z=10$, $z=15$ (depth of the lower edge of the fault), and $z=20$ km. The pattern of S_{xy}, which represents the change in the tectonic shear stress induced by faulting, is practically the same at all depths between the upper edge and the lower edge of the fault.

The contour maps of S_{xy} in the horizontal plane $z=10$ km are shown in Fig. 2. The values of contours are given in units of the rigidity modulus of the medium, μ. The positive values of S_{xy} indicate an increase of tectonic shear stress while negative values correspond to a relief of the tectonic stress as a result of faulting. As can be seen from Fig. 2, S_{xy} is symmetric with respect to x and y and its negative values prevail around the fault except for the regions beyond the ends of the fault. The positive values of S_{xy}, of smaller amplitude, appear also in the regions off the fault plane. The pattern of S_{xy} shown in Fig. 2 is very similar to that in the ground surface, as obtained by CHINNERY (1963) for the case of a vertical strike-slip fault in semi-infinite medium. The contour maps of S_{xy} in planes below the lower edge of the fault ($z>15$ km, not shown in figures) are of a different character in the regions adjacent to the fault. At these depths, S_{xy} takes only positive values in the fault vicinity so the regions of negative values of S_{xy} become separated. Farther away from the fault the patterns of the computed S_{xy} are similar for all depths.

All remarks regarding dependence of stress on depth, which was stated above in relation to the S_{xy} component, remain valid for normal stress component S_{yy} as well. Fig. 3 shows the contour lines of S_{yy} at a 10 km depth, which are representative for all depths. S_{yy} is anti-symmetric with respect to x and y so it is equal to zero in the fault plane (plane $y=0$) and in the plane perpendicular to it, passing through the middle of the fault (plane $x=0$). The positive and negative values

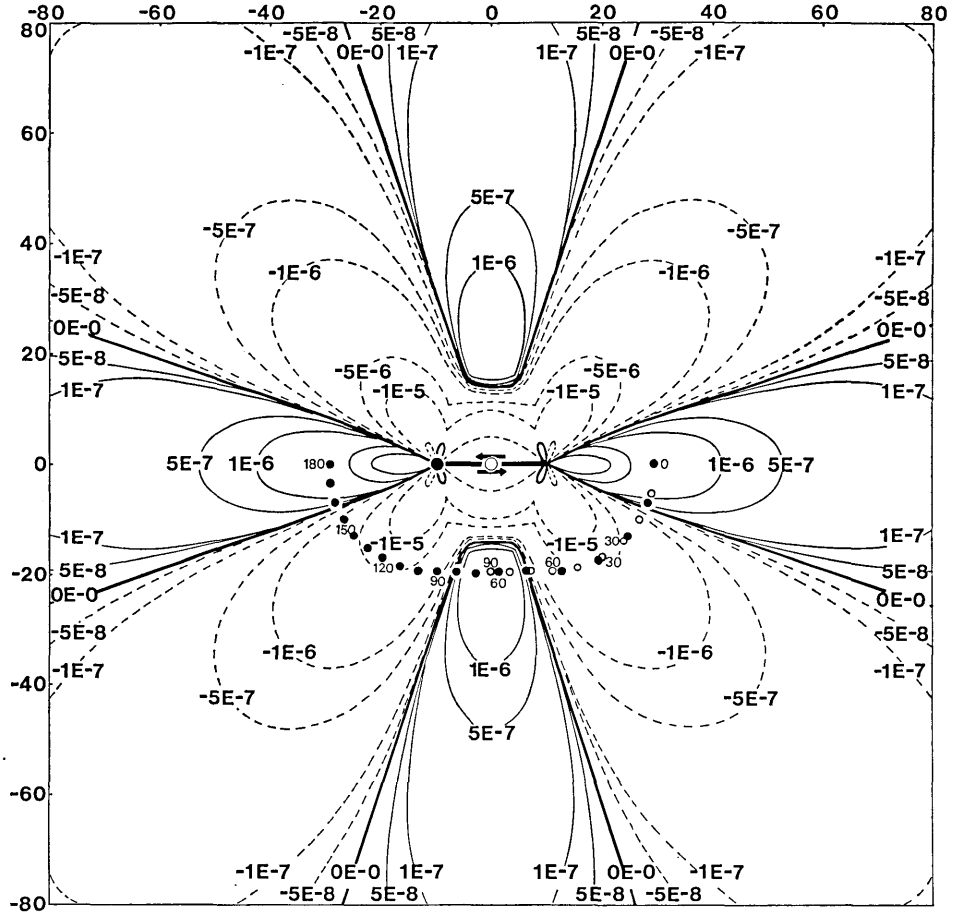

Fig. 2. Contour lines within the square region with a side 160 km in the horizontal plane $z=10$ km for the S_{xy} component of stress change induced by a vertical strike-slip fault 20 km long and 15 km wide. The contour values are given in units of the rigidity modulus μ. The empty and solid circles around the fault (thick line) indicate sites at which the dynamic stress synthetics shown in Figs. 6-9 were computed. Solid and empty circles are asssociated with unilateral and bilateral ruptures, respectively. Numbers alongside the circles indicate the values of the angle θ.

indicate tension and compression, respectively. Comparing the pattern of S_{yy} (Fig. 3) with that of S_{xy} (Fig. 2), it is readily seen that, in some regions off the fault, the former component varies in space (change sign) to even a greater extent than the latter.

b. Static resultant stress in the semi-infinite medium

In order to estimate how faulting in the medium affect stability of adjacent faults parallel to the plane $y=0$, it is necessary to take

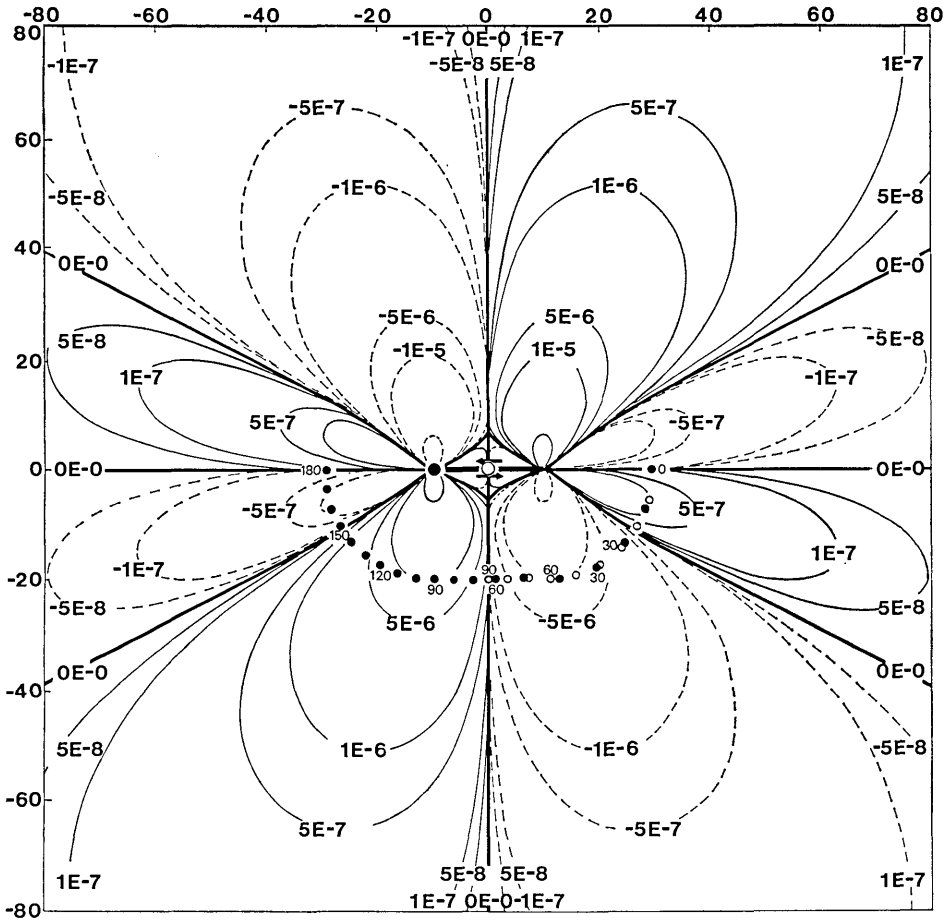

Fig. 3. Same as Fig. 2 for the S_{yy} component.

into consideration all three components of the stress vector, S_{xy}, S_{yy}, and S_{zy}, acting across the supposed potential fault surfaces. Among them, however, the S_{xy} component plays a major role in the analysis. We assume that the tectonic shear stress is uniform in the space, and the tectonic shear stress is uniform in the space, and the pattern of the contour lines of S_{xy} quantitatively indicates in which areas there is an increase and decrease of the tectonic stress due to faulting. We may then suppose that further material failure is more likely to occur in the regions of positive values of S_{xy}, whereas the potentially active faults located in the regions of negative values of S_{xy} should become more stable after the source faulting.

On the other hand, the change in the normal stress component S_{yy} should influence the stability of any potential fault as well, since it

affects the frictional resistance on the fault surface. According to the sign convention adapted here, regions of positive (negative) values of S_{yy} correspond to those where compression acting on faults decreases (increases) and the probability of further faulting becomes greater (smaller). As for the S_{zy} component, we do not take it into account in the present analysis. The absolute values of S_{zy} are, on the average, much smaller than those of the S_{xy} and S_{yy} components.

In order to estimate quantitatively what is the resultant effect of faulting on stability of nearby faults, we applied the experimental results pertaining to friction on faults (BYERLY, 1978). It was found that the function which relates the normal stress σ_n in the range $2kb<\sigma_n<20kb$ (which corresponds roughly to the presumed range of compressive stress for crustal earthquakes) with the shear stress required to cause sliding on faults is approximately given by the linear equation

$$\tau=0.5+0.6\cdot\sigma_n.$$

Using this result we propose the quantity

$$S_r=S_{xy}+0.6\cdot S_{yy},$$

which we call the resultant stress to be applied as a single parameter describing the effect of faulting in the medium on stability of adjacent faults. STEIN and LISOWSKI (1983) independently introduced the similar quantity with a different coefficient. They called the value as "Coulomb criteria" and evaluated it at the ground surface to apply to shallow aftershocks.

Figures 4 and 5 show contour lines of S_r in the horizontal planes $z=10$ and $z=20$ km, respectively. Here, we used a semi-infinite medium model so that the obtained result could be compared to the observed surface strain change due to an earthquake. The pattern of S_r in the plane $z=10$ km is representative for the range of depths from the ground surface to the depth of the lower edge of the fault ($z=15$ km). Furthermore, we can consider the depth of 10 km as characteristic for the so-called seismogenic layer (zone where most of crustal earthquakes initiate). Consequently, we can assume that the results regarding the stress change at this depth are of greatest importance in the analysis of fault stability.

As can be seen from Fig. 4, there are four separate regions around the fault where the resultant stress takes on positive values. The pattern, as a whole, is symmetric with respect to the origin of the coordinate. The four line segments along where the resultant stress reachs the greatest positive values pass through both of the edges of the fault. Two of these lines, which extend farther off both edges of

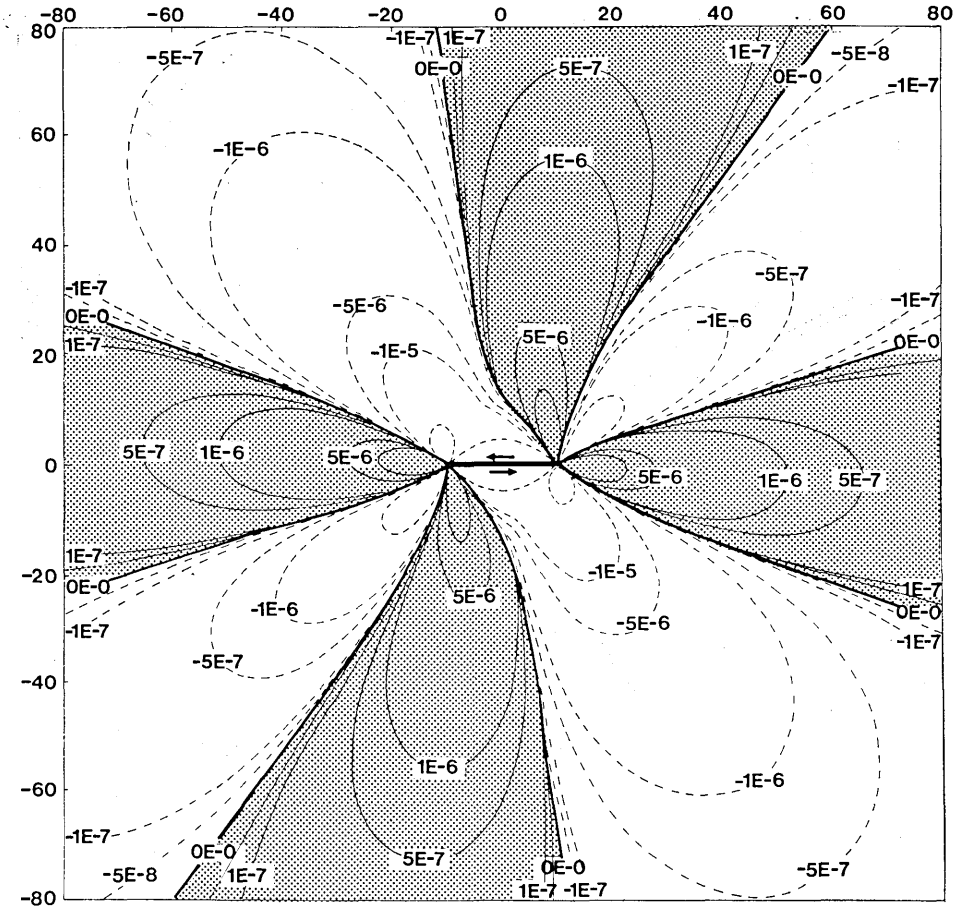

Fig. 4. Contour lines for the resultant stress S_r in the horizontal plane $z=10$ km. The contour values are given in units of μ. Stippled regions indicate regions where probability of further faulting increases.

the fault, are nearly straight lines with invisibly slight curvature. The remaining two lines are curved convex to the plane perpendicular to the fault. It should be noted that the average values of positive S_r for the regions which are off the fault plane are greater than those in regions adjacent to the fault plane.

The pattern of S_r in the planes below the depth of the lower edge of the fault differs from that at depths above it for the regions close to the fault (Fig. 5). In the latter regions the resultant stress takes positive values only. Farther away from the fault the patterns of S_r in horizontal planes above and below the lower edge of the fault are similar except that the absolute values of S_r in the former case are greater than in the latter.

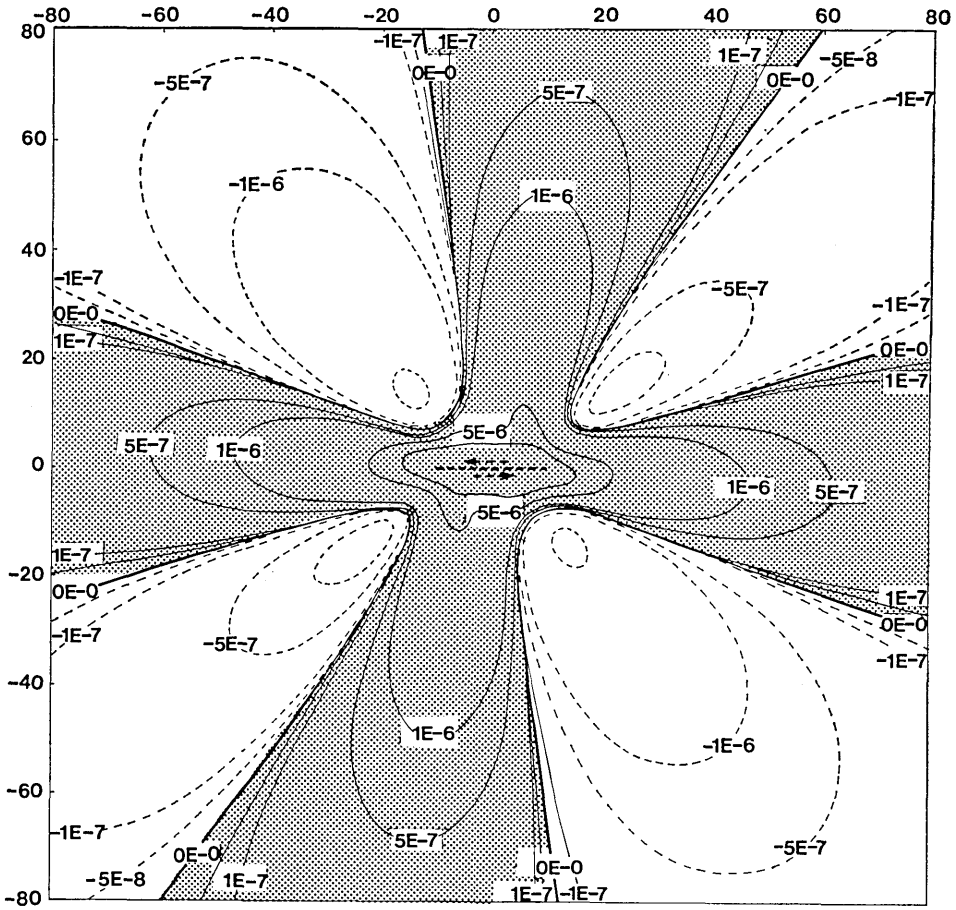

Fig. 5. Contour lines of S_r in the horizontal plane $z=20$ km. See the caption for Fig. 4 for other details.

c. Dynamic stress in the infinite medium

The dynamic stress induced by faulting was calculated for different points surrounding the fault in horizontal planes $z=10$, $z=15$, and $z=20$ km in the infinite medium. The observation points were chosen to be located at equal distances of 20 and 40 km from the nearest point of the fault. Figures 6, 7, and 8 show the synthetic stress components S_{xy} (continuous lines), S_{yy} (broken lines), and S_{zy} (dashed lines) computed at different sites (different values of angle θ—see Fig. 1b) for the case of bilateral and unilateral ruptures, respectively. The sites are located at a distance of 20 km from the fault in the horizontal plane $z=10$ km. The positions of the observation points in relation to the fault (solid circles—unilateral rupture, empty circles—bilateral rupture) are shown in Figs. 2 and 3, from which the corresponding static values of stress

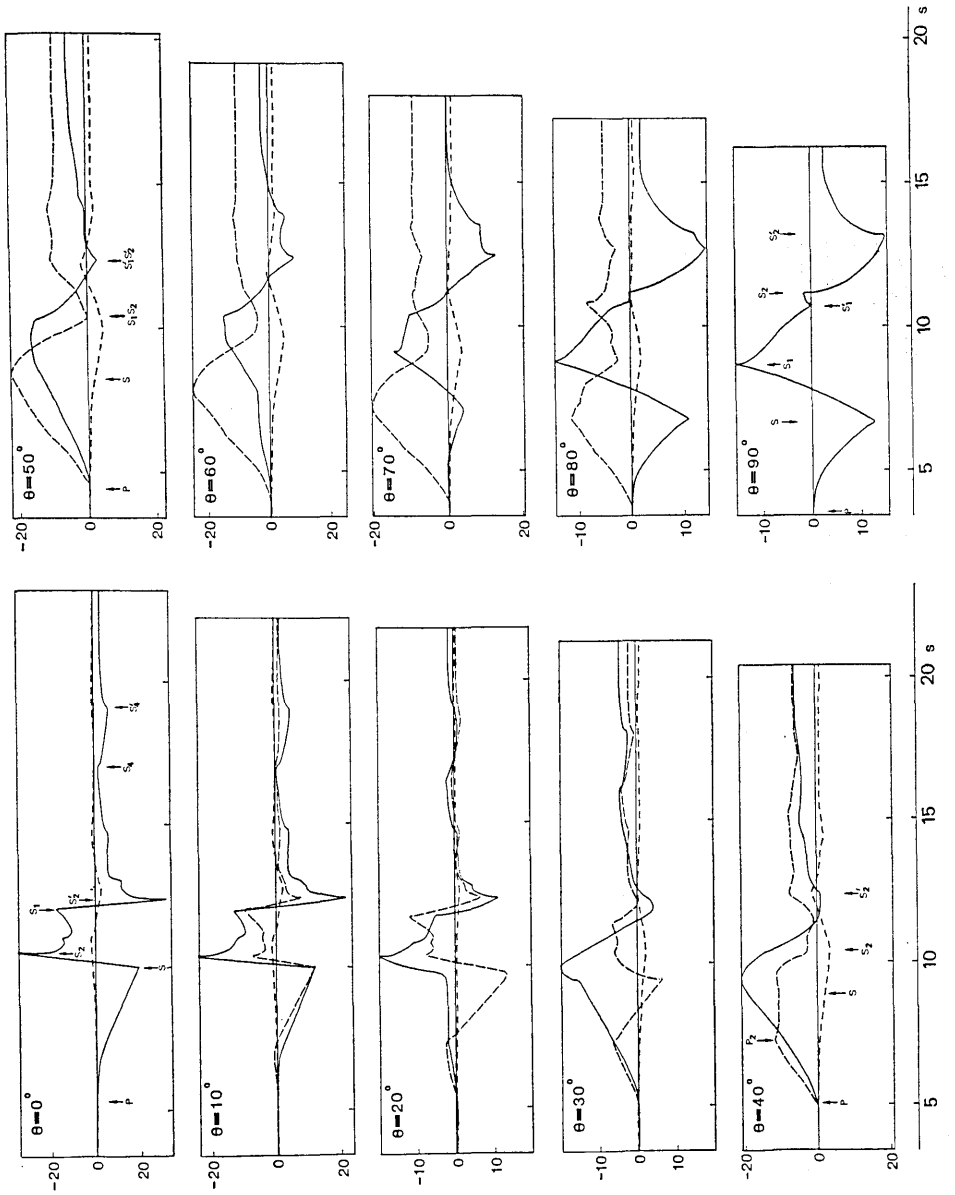

Fig. 6. Dynamic stress induced by the vertical strike-slip fault for bilateral ruptures. Continuous, broken, and dashed lines indicate S_{xy}, S_{yy}, and S_{zy} components of stress, respectively. Synthetics are computed at sites in the horizontal plane $z=10$ km at a distance of 20 km from the fault. The position of the sites which is indicated by the values of the angle θ is shown in Figs. 2 and 3. The vertical (stress) and horizontal (time) scales are in units of $\mu\times10^{-6}$, and in seconds, respectively. The arrows and the symbols standing by indicate P- and S- wave arrivals, as well as arrivals of different stopping phases.

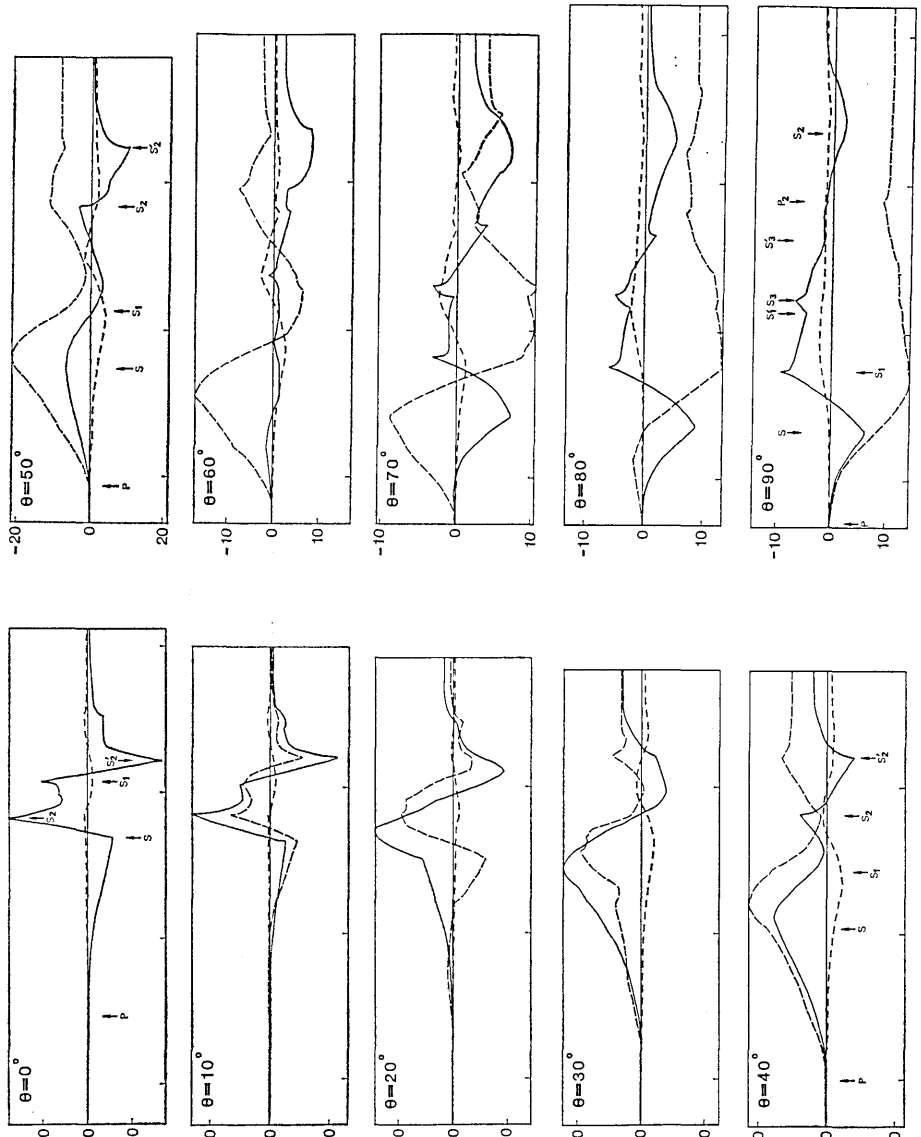

Fig. 7. Synthetics computed for the case of unilateral rupture at sites located in the horizontal plane $z=10$ km at the distance of 20 km from the fault for different values of the angle θ in the range 0°–90°. See the caption for Fig. 6 for other datails.

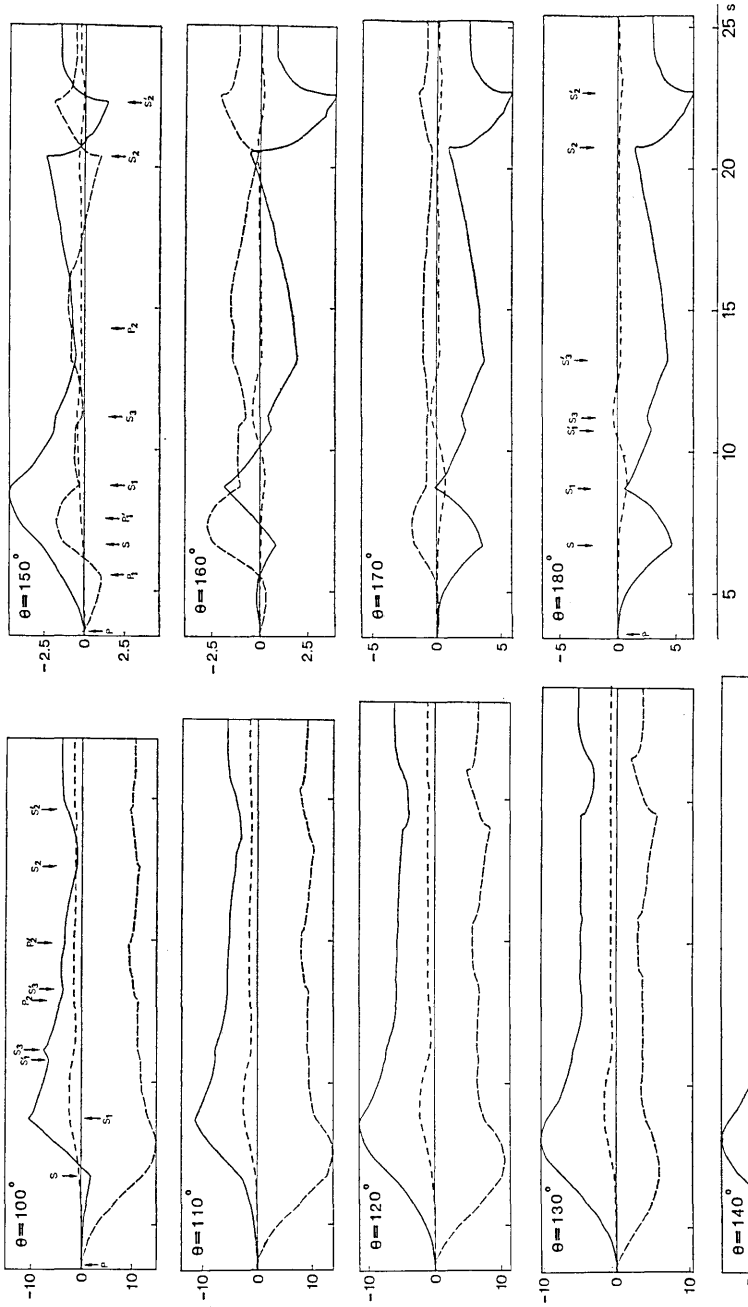

Fig. 8. Same as Fig. 7 at sites with different values of the angle θ in the range 100°–180°

components S_{xy} and S_{yy} can be found approximately. Due to the symmetry of the stress field, it is sufficient to compute the stress components S_{xy}, S_{yy}, and S_{zy} only for the first quadrant ($0° \leq \theta \leq 90°$) in the case of a bilateral rupture, and for the first and second quadrants ($0° < 180°$) in the case of a unilateral rupture. The dynamic stress has the same symmetry properties with respect to x and y (bilateral rupture) and with respect to y (unilateral rupture) as the static stress discussed above. This means that the corresponding synthetics in the remaining quadrants are either the same or of different polarity only. The amplitude of synthetics at each observation point is normalized to the greatest maximum value of S_{xy}, S_{yy}, and S_{zy} (whichever is the greatest) at this point. Amplitudes of stress are given in units of $\mu \times 10^{-6}$.

The major phases of stress synthetics can be associated with arrivals of P- and S-waves from the initial point of rupture and with P- and S- stopping phases (SAVAGE 1965, 1966; RYBICKI, 1976). For the present model of faulting there exist, in general, four stopping phases (both P and S) when the rupture starts from within the fault (bilateral rupture), and three stopping phases when the hypocenter is located at the edge of the fault (unilateral rupture). The stopping phases associated with the edges: $z=W$, $x=L/2$, $z=0$, and $x=-L/2$ (Fig. 1a) are denoted as P_1, S_1; P_2, S_2; P_3, S_3; P_4, S_4; respectively. In the case of a unilateral rupture the stopping phases P_4 and S_4 do not exist. Since we are assuming that the source time function is of the ramp type with the rise time $t_0=2$s, each stopping phase splits into two subphases separated by the time interval of 2s. Each second subphase is denoted by the prime mark. Only some major stopping phases are indicated in Figs. 6–8. The arrival times of different stopping phases depend on the position of the observer. As it can be intuitively expected, the P-stopping phases are apparent only for the normal stress component S_{yy}. We also note that, on the average, the stopping phases manifest themselves much more distinctly for synthetics at sites located 40 km away from the fault (not shown in figures).

When discussing the general characteristics of the dynamic stress field due to faulting, it is useful to take the corresponding static values as a reference signal. (The static value of stress at any point is reached when the signal from the furthermost point undergoing slip has arrived at the observer.) As is readily seen from Figs. 6–8, the dynamic stress components S_{xy}, S_{yy}, and S_{zy} have a different character depending on the angle θ between the fault plane and the line joining the observer with the coordinate origin. For the fixed value of

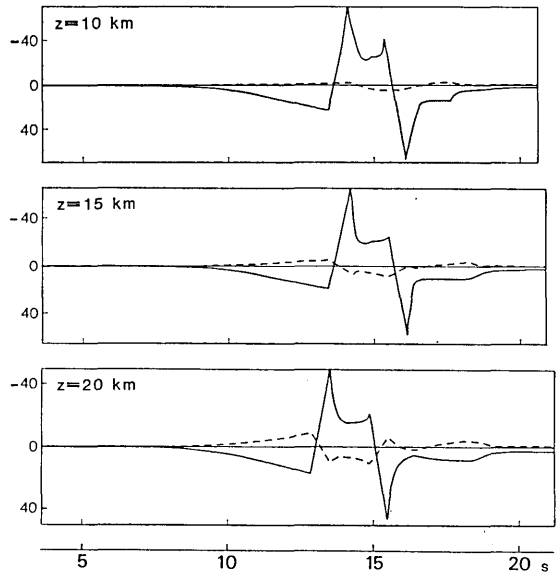

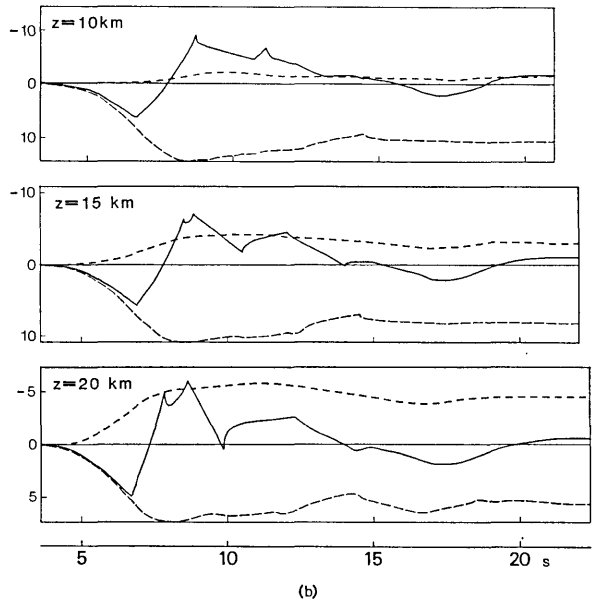

Fig. 9. Synthetics computed for cases of unilateral rupture at sites located at a distance of 20 km from the fault for (a) $\theta=0°$, and (b) $\theta=90°$, for three different depth: 10, 15, and 20 km. See the caption for Fig. 6 for other details.

θ, however, the form of synthetics calculated at different distances from the fault and at different depths does not change in such a

substantial way. As an example, the synthetics computed at sites located at three different depths for $\theta=0°$ and $\theta=90°$ at the distance of 20 km from the fault for a case of unilateral rupture are shown in Fig. 9.

Clearly, a strong directivity effect (BEN-MENAHEM and SINGH, 1981), which is visible especially in the case of a unilateral rupture, is one of the most distinctive traits of the dynamic stress field. This effect is most striking for the S_{xy} component in which the maximum amplitudes (both positive and negative values) in the direction $\theta=0°$ are greatest both in terms of absolute values as well in terms of relative values in relation to corresponding values of static stress. The ratio of maximum amplitude of dynamic stress to the static stress is, on the average, greater for the S_{xy} component than for the S_{yy} and S_{zy} components.

The dynamic stress component S_{yy} is equal to zero in the plane $y=0$ (fault plane) which to some extent masks the directivity effect for this component. The greatest amplitudes of S_{yy} appear in the regions where the absolute value of the static stress are also dominant. In these regions, the maximum dynamic values of S_{yy} exceed those of the S_{xy} and S_{zy} components.

The dynamic values of S_{zy} stress components are much smaller than those of the two remaining components of the stress vector. The maximum amplitudes of S_{zy} become comparable with those of S_{xy} and S_{yy} in the same regions in the vicinity of the corners of the fault where the S_{zy} component of static stress takes on relatively high values.

Apparently there is a general correlation between the form of stress synthetics and the corresponding values of static stress. Among others, it seems that for all synthetics the average value of the dynamic stess is equal to the static stress. This result should be verified by a more comprehensive theoretical analysis.

d. Dynamic resultant stress in the infinite medium

In order to estimate quantitatively what is the effective dynamic perturbation in stability of the adjacent faults due to slip on the source fault, we calculated the maximum positive dynamic values of the resultant stress S_r defined previously. This quantity specifies the upper limit of the resultant stress increase imposed on neighboring faults as a result of fracture on the given fault. The maximum positive values of S_r for bilateral and unilateral rupture models in the plane $z=10$ km at distances of 20 and 40 km from the fault are shown in Fig. 10. The corresponding patterns of maximum positive values of S_r in the planes $z=15$ and $z=20$ km are similar to those in the plane $z=10$ km.

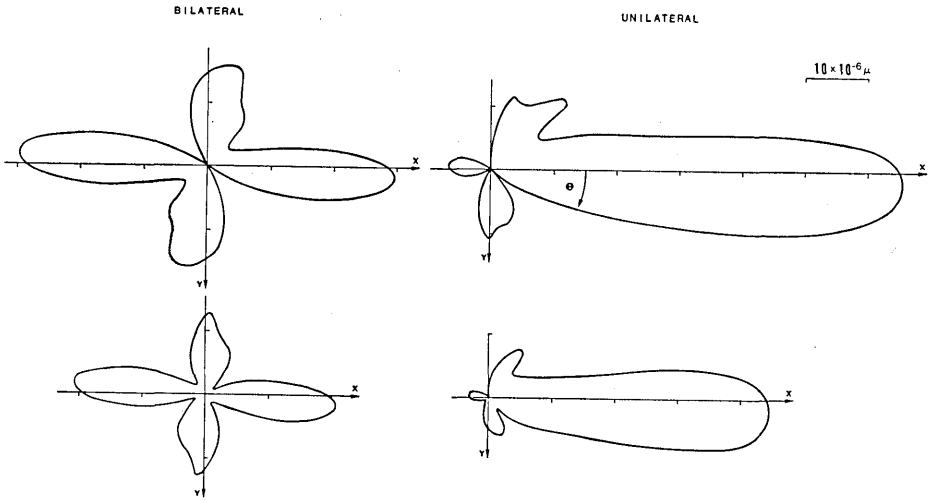

Fig. 10. Maximum positive values of the dynamic resultant stress $S_r(t)$ for bilateral and unilateral rupture in the plane $z=10$ km at distances from the fault equal to 20 (upper part) and 40 km (lower part).

The patterns of maximum dynamic positive values of S_r (Fig. 10) together with that showing the contour lines of static values of S_r (Fig. 4) is another clear example of directivity effect and of apparent correlation between the dynamic and static stress field. The maximum positive dynamic values of S_r are the greatest in the direction close to the direction of slip (more exactly the angle between these two directions is about 3–4°). The high amplitudes of the dynamic resultant stress are narrowly concentrated around this direction and slowly diminish with distance from the fault. For example, we may note that the maximum positive amplitudes of S_r at a distance of 20 km from the fault for the direction which makes the angle only a little more than 10° with the direction along which positive dynamic values of S_r are the greatest, are smaller than those at a distance of 40 km from the fault for the direction of maximum stress concentration.

Assuming the value of the rigidity modulus as equal to 2.5×10^{11} cgs, the maximum positive values of S_r are equal to about 16 and 11 bars at distances of 20 and 40 km from the nearest point of the fault in the case of a unilateral rupture, and 7.5 and 5 bars for the same distances in the case of a bilateral rupture, respectively.

It should be noted that the resultant dynamic stress $S_r(t)$ takes frequently positive values in some time intervals at sites where the corresponding static values of S_r are negative. The regions where $S_r(t)$ is completely negative are associated with those where the corresponding static stress takes high negative values.

4. Discussion and Conclusions

The foregoing considerations enabled us to get the general characteristics of the static and dynamic stress field induced by faulting in the medium. The main purpose of this study is to apply these results to assess the stability of potentially active faults located in the vicinity of the source fault. The following two questions are of greatest importance in such an analysis: (1) in which areas around the source fault does the probability of further fracture increase, and (2) how high is the increase of dynamic and static stress in these areas. In order to answer these questions we introduced a parameter called the resultant stress. This quantity, which contains both shear and normal components of the stress vector, was taken on the basis of the results of laboratory experiments of fault friction. The distribution of the static and dynamic resultant stress around the source fault of a vertical strike-slip type suggests the existence of four regions where the stability of parallel, potentially active faults is decreased as a result of faulting. Two of them are located in the vicinity of the fault plane and on the extention of the fault, while two others extend off the fault plane. It should be noted that the magnitude of the resultant static stress is, on the average, higher in the latter regions than in the former. Such stress distribution applies approximately for the depth range from the ground surface to a depth below that of the seismogenic layer.

The dynamic stress—as a function of time—was computed at selected points around the source fault. The complex form of synthetics can be interpreted in terms of *P*- and *S*- wave phases arriving from the initial point of fracture and of stopping phases of fracture at the respective edges of the fault. The dynamic peak amplitude is, on the average, several times higher than the corresponding static stress value. There exists a kind of correlation between the form of synthetic dynamic stress and its static value. In particular, the average value of dynamic stress at any observation site seems to be equal to the corresponding static value. A strong directivity effect is another characteristic feature of the dynamic stress field. The maximum peak values of the dynamic stress are more than one order of magnitude higher than the corresponding static ones, reaching the values of the order of 10 bars or even more at distances comparable to the fault's dimension in the case of fault models that are comparable to magnitude 7 earthquakes.

It is beyond the scope of the present paper to analyse how the dynamic stress may influence other active faults that are under a critical stress condition. This problem is left for future study. Such

study is necessary in order to develop a useful and reliable technique for the assessment of stability of a potential active fault. It seems advantageous, however, to examine basic assumptions taken in the present paper and to discuss briefly some problems related to the results obtained. They can be summarized as follows:

(1) The infinite space model which was used to evaluate the dynamic stress field is definitely a drastic simplification, although not necessarily an oversimplification, as far as the present approximation is concerned. We were interested here only in finding general features of a near field (distance comparable to the fault dimension) at the depth comparable to that of the seismogenic layer so the influence of the free surface should not be very dramatic. In a more precise model, however, the present assumption should be reconsidered.

(2) The assumption concerning homogeneity of the medium and of the initial tectonic stress field must be improved for a more realistic model. The earth's crust in seismotectonic areas has very inhomogeneous structures containing numerous fractures. It is evident that such a complex medium structure should affect the spatial distribution of the stress field as well. At least gross inhomogeneities of the medium ought to be taken into account in a more realistic model.

(3) As the results obtained indicate, the problem of how the transient stress affects the strength of the material is of great importance when considering the stability of faults. The dynamic stress peak values may be ten or more times higher than the corresponding static stress, and the greatest peak values are associated with impulses of the shortest duration. These results give rise to questions regarding the time interval which is necessary to cause fracture on a fault under the assumption that "the static strength" is only temporarily exceeded. (By "the static strength" we understand here the strength for stress slowly increasing with time.) Further laboratory and theoretical studies are indispensable in this respect.

(4) Suppose that a potentially active fault is subject to known seismic disturbances and remain unmoved. Suppose also that a proper technique which would take into account the necessary reduction for the time-dependence effect on strength and the annual rate of stress increase is developed. Then it would be possible to estimate the minimum time period before the next fracture, i.e. we would be able to get information about actual fault stability. The development of such technique and further study regarding mechanical interaction between the neighboring active faults seems to be a task which is of great importance for long-term earthquke prediction.

Acknowledgments

We are grateful to Prof. R. Sato, Drs. T. Iwasaki and Y. Suzuki for valuable discussions and for offering us the computer programs which were used in the present study. We profited also very much from discussions with Profs. T. Maruyama, T. Mikumo, M. Ohnaka and Dr. T. Miyatake.

We are thankful for help in the preparation of the manuscript to Ms. M. Hirai and Mr. S. Matsumoto. Dr. R. McCabe read the manuscript and offered valuable comment and advice.

This research was conducted during the stay of one of the authors (K. R.) in Japan in the frame of cooperation between the Japan Society for the Promotion of Science and the Polish Academy of Sciences. The support of the Japan Society for the Promotion of Science is gratefully acknowledged.

References

BEN-MENAHEM, A. and S. J. SINGH, 1981, *Seismic waves and sources*, Springer, New York, 1108 pp.

BYERLY, J., 1978, Friction of rocks, *Pageoph*, **116**, 615-626.

CHINNERY, M. A., 1963, The stress changes that accompany strike-slip faulting, *Bull. Seism. Soc. Amer.*, **53**, 921-932.

CHINNERY, M. A., 1966a, Secondary faulting, 1. Theoretical aspects, *Can. J. Earth Sci.*, **3**, 163-174.

CHINNERY, M. A., 1966b, Secondary faulting, 2. Geological aspects, *Can. J. Earth Sci.*, **3**, 175-190.

DAS, S. and C. H. SCHOLZ, 1981, Examples and possible explanation for occasionally observed clusters of off-fault aftershocks, *Bull. Seism. Soc. Amer.*, **71**, 1669-1675.

IWASAKI, T., 1978, Theoretical strain seismograms due to moving fault in an infinite medium (in Japanese), Master's Thesis, Faculty of Science, University of Tokyo.

IWASAKI, T. and R. SATO, 1979, Strain field in a simi-infinite medium due to an inclined rectangular fault, *J. Phys. Earth*, **27**, 285-314.

MATSUDA, T., 1975, Magnitude and recurrence interval of earthquakes from a fault (in Japanese), *Zisin*, **28**, 269-283.

MATSUDA, T., 1977, Estimation of future destructive earthquakes from active faults on land in Japan, *J. Phys. Earth*, **25**, Suppl., S251-S260.

NIEWIADOMSKI, J. and K. RYBICKI, 1984, The stress field induced by antiplane shear cracks—Application to earthquake study, *Bull. Earthq. Res. Inst., Univ. Tokyo*, **59**, 67-81.

RESEARCH GROUP FOR ACTIVE FAULTS, 1980, *Active faults in Japan: sheets, maps, and inventories*, University of Tokyo Press, Tokyo, 363 pp.

RYBICKI, K., 1976, Far-field body waves generated by slip faulting: case of an elliptically expanding rupture, *J. Phys. Earth*, **24**, 313-339.

SATO, R., 1975, Fast computation of theoretical seismograms for an infinite medium, Part I. Rectangular fault, *J. Phys. Earth*, **23**, 323-331.

SATO, R., 1976, Fast computation of theoretical seismograms for an infinite medium, Part II. Fault with an arbitrary shape, *J. Phys. Earth*, **24**, 43-49.

SAVAGE, J. C., 1965, The stopping phase on seismograms, *Bull. Seism. Soc. Amer.*, **55**, 47-58.

SAVAGE, J. C., 1966, Radiation from a realistic model of faulting, *Bull. Seism. Soc. Amer.*, **56**, 577-592.

SAVAGE, J. C. and M. M. CLARK, 1982, Magmatic resurgence in Long Valley caldera, California: Possible cause of the 1980 Mammoth Lakes earthquakes, *Science*, **217**, 531-533.

SMITH, S. W. and W. VAN DE LINDT, 1969, Strain adjustments associated with earthquakes in Southern California, *Bull. Seism. Soc. Amer.*, **59**, 1569-1589.

STEIN, R. S., 1984, Implication of off-fault aftershocks for preearthquake stress, *Proceedings of International Symposium on Recent Crustal Movements of the Pacific Region*, Wellington, New Zealand, February 1984, in Press.

STEIN, R. S. and M. LISOWSKI, 1983, The 1979 Homestead Valley earthquake sequence, California: Control of aftershocks and postseismic deformation, *J. Geophys. Res.*, **88**, 6477-6490.

YAMASHINA, K., 1978, Induced earthquakes in the Izu Peninsula by the Izu-Hanto-Oki earthquake of 1974, Japan, *Tectonophysics*, **51**, 139-154.

活断層の相互力学作用
——断層運動による静的・動的応力場——

東京大学地震研究所 Kacper RYBICKI, 加藤照之, 笠原慶一

活断層の安定性を考えるてがかりとして，隣接断層の運動によってどのような静的・動的応力がかかるかを調べてみた．断層運動のモデルには，無限あるいは半無限の均質媒質内の垂直面に沿って，横ずれ性の Volterra 型くい違いが起きることを考える．

こうした断層運動が，それに平行な他の断層の安定性にどのような力学効果を与えるか．それを定量的に見積もるため，摩擦の室内実験を参考にして，新たなスカラー量を定義しよう．この量，すなわち合成応力 (resultant stress) は，断層面に作用する剪断・法線両応力成分を組み合わせたものである．地震多発層 (seismogenic layer) に相当する深度に沿ってこの合成応力の方位分布を見ると，それが大きい．すなわち破壊が起こりやすいと思われる領域が断層の周りに四つあることがわかる．そのうち二領域は断層線の延長上に位置し，他の二つは断層から横に延びている．後者は断層の中央でそれに直交する面に関して非対称であることが注目される．破壊がさらに起きるとすれば，その確率は断層周辺のこれら領域で若干高いのではなかろうか．

動的応力場には指向性が現れる特徴があり，特に単方向性 (unilateral) 破壊の場合に著しい．その分布は，また，静的応力場ともよく対応している．ここで動的な合成応力の最大値は，$M7$ 程度の地震に相当する断層モデルを仮定した場合，断層からその長さ程度離れたところで 10 bar くらいと見られる．ちなみに最大動的応力の最大静的応力に対する比は，観測点位置や破壊伝播特性によるけれども，2.3 から 50 くらいの間にある．隣接断層が受ける動的応力はこのように大きなものであるが，その力学効果を評価するためには，過渡的応力に対する断層強度の時間効果をさらに解明する必要があろう．